DOI: 10.6060/ivkkt.20216407.6409

УДК: 537.528+541.15

ПЛАЗМА-РАСТВОРНЫЙ СИНТЕЗ ОКСИДА ЖЕЛЕЗА (III)

К.В. Смирнова, Д.А. Шутов, А.Н. Иванов, А.С. Манукян, В.В. Рыбкин

Кристина Валерьевна Смирнова, Дмитрий Александрович Шутов, Александр Николаевич Иванов, Анна Славиковна Манукян, Владимир Владимирович Рыбкин *

Кафедра приборов и материалов электронной техники, Ивановский государственный химико-технологический университет, Шереметевский пр., 7, Иваново, Российская Федерация, 153000
E mail: ivkkt@isuct.ru, rybkin@isuct.ru*

Исследован процесс образования нерастворимых соединений железа, инициируемый действием разряда постоянного тока атмосферного давления в воздухе на водный раствор сульфата железа (III). Было обнаружено, что, когда раствор является анодом, действие разряда приводит к образованию коллоидного раствора гидроксосульфатов железа и гидроксида железа. Коллоидный раствор, как показывает метод DLS, состоит из двух фракций размером 47 нм (73%) и 950 нм. Кинетику образования коллоидных частиц исследовали турбодиметрическим методом. Оказалось, что скорость образования увеличивается с увеличением тока разряда от 30 до 70 мА. При концентрации сульфата железа (III) 5 ммоль/л константа скорости процесса увеличивается с $7 \cdot 10^{-3}$ до $2{,}2 \cdot 10^{-2}$ $с^{-1}$. При разрушении этого раствора образуется осадок соответствующих соединений. Рентгеноструктурный анализ показал, что осадок аморфный. Полученный осадок, как показывает СЭМ, имеет плотную структуру. Размер частиц в среднем составляет 100 нм. В результате прокаливания осадка, как показали рентгеноструктурный анализ и EDX, он превращается в кристаллический оксид железа (III) тригональной системы (гематит). Полученный оксидный порошок имеет развитую поверхность со средним размером частиц менее 50 нм.

Ключевые слова: газовый разряд, оксид железа, коллоидный раствор, СЭМ, рентгеновский анализ, ДРС, ЕДС

PLASMA-SOLUTION SYNTHESIS OF IRON (III) OXIDE

K.V. Smirnova, D.A. Shutov, A.N. Ivanov, A.S. Manukyan, V.V. Rybkin

Kristina V. Smrnova, Dmitriy A. Shutov, Aleksandr N. Ivanov, Anna S. Manukyan, Vladimir V. Rybkin*

Department of Electronic Devices and Materials, Ivanovo State University of Chemistry and Technology, Sheremetevskiy ave., 7, Ivanovo, 153000, Russia
E mail: ivkkt@isuct.ru, rybkin@isuct.ru*

The process of formation of insoluble iron compounds, initiated by the action of a direct current discharge of atmospheric pressure in air on an aqueous solution of iron (III) sulfate, has been investigated. It was found that when the solution is the anode, the action of the discharge leads to the formation of a colloidal solution of iron hydroxosulfates and iron hydroxide. The colloidal solution, as shown by the DLS method, consists of two fractions 47 nm (73%) and 950 nm in size. The kinetics of the formation of colloidal particles was investigated by the turbodimetric method. It turned out that the rate of formation increases with an increase in the discharge current from 30 to 70 mA. At concentrations of iron (III) sulfate 5 mmol/l the rate constant of the process increases from $7 \cdot 10^{-3}$ to $2.2 \cdot 10^{-2}$ s^{-1}. When this solution is destroyed, a precipitate of the corresponding compounds is formed. X-ray analysis showed that the precipitate is amorphous. The resulting precipitate, as shown by SEM, has a dense structure. The particle size is 100 nm on average. As a result of calcining the precipitate, as shown by X-ray analysis and EDX, it turns into crystalline iron (III) oxide of the trigonal system (hematite). The resulting oxide powder has a developed surface, with a particle size of less than 50 nm on average.

Key words: gas discharge, iron oxide, colloidal solution, SEM, X-ray, DLS, EDX

Для цитирования:
Смирнова К.В., Шутов Д.А., Иванов А.Н., Манукян А.С., Рыбкин В.В. Плазма-растворный синтез оксида железа (III). *Изв. вузов. Химия и хим. технология*. 2021. Т. 64. Вып. 7. С. 83–88
For citation:
Smirnova K.V., Shutov D.A., Ivanov A.N., Manukyan A.S., Rybkin V.V. Plasma-solution synthesis of iron (III) oxide. *ChemChemTech* [*Izv. Vyssh. Uchebn. Zaved. Khim. Khim. Tekhnol.*]. 2021. V. 64. N 7. P. 83–88

INTRODUCTION

Iron oxides are one of the most technically significant transition metal oxides. Iron oxide-based materials are widely used as catalysts for various chemical processes. For example, iron oxides are good catalysts for the processes of the release of molecular oxygen from water, the oxidation of organic molecules, the release of chlorine, the breakdown of water, the reduction of oxygen, and the decomposition of hydrogen peroxide [1]. Nanodispersed iron oxide powders are used for the selective catalytic reduction of nitrogen oxides NO and NO_2 with ammonia [2]. This reaction underlies the cleaning of exhaust gases from diesel engines. Iron oxides have been used as pigments for millennia. Creation of nanosized oxide pigments greatly expanded range of applications [3]. Therefore, in recent years there were many studies on the synthesis of iron oxides using a variety of methods of chemical deposition, mechanical grinding, and physical–chemical methods (hydrothermal, electrochemical, aerosol, chemical and metallurgical, etc.). The main drawback of the above methods is that they either require a large number of reagents that by the nature of things contaminate the final product, or they are practically and technically sophisticated.

Recently, for the synthesis of nanomaterials, it is proposed to use the processes occurring in a solution under the action of plasma [4]. In this way, nanoparticles of metals, alloys, oxides, and a number of composite materials were synthesized [5].

In particular, zinc, cadmium and manganese oxides were synthesized in works [6-8]. Information on the formation of oxygen-containing iron compounds upon exposure to discharges in aqueous solutions is extremely limited. Thus, in [9], the formation of yellow-brown suspensions was noted under the action of a DC discharge in helium on a $FeCl_2$ solution. Data on the kinetics of synthesis, chemical and crystal structure of compounds, particle sizes are not provided. It is only noted that the resulting particles include iron and oxygen (EDX analysis). In [10], the effect of a diaphragm discharge on an aqueous solution of $FeCl_3$ was studied. The authors observed a decrease in the concentration of Fe^{3+} ions and the formation of a precipitate a in the region of the diaphragm. No information is provided on the kinetics of the process and properties of the precipitate. It was shown in work [8] that the effect of a discharge on a solution of iron (II) nitrate leads to the reduction of iron (II) to iron (III) with the formation of colloidal solutions of iron (III) hydroxo compounds. When these compounds are calcined, crystalline Fe_2O_3 is formed in the γ form. The transformation of soluble iron salts into insoluble salts also has an important ecological aspect. Almost all groundwater sources contain impurities of iron ions, which must be removed.

This article studies the processes occurring under the action of a direct current discharge of atmospheric pressure in air on aqueous solutions of iron (III) sulfate. When the discharge acts on the solution, a colloidal solution is formed, the decomposition of which results in a precipitate. The kinetics of the formation of colloidal particles, their size and particle size of the sediment, as well as its chemical and phase composition have been studied.

EXPERIMENTAL PART

The solutions were prepared by dissolving iron sulfate $Fe_2(SO_4)_3 \cdot 9H_2O$ of analiticaql grade in distilled water. The initial concentration of the solution varied in the range of 2.5-5 mmol/l.

The discharge cell consisted of two identical cylindrical communicating vessels, which were separated by a cellophane membrane. The volume of each cell was 100 ml. Two titanium electrodes were located in the center of each cell at a distance of 5 mm from the solution surface. That is, two discharges burned in the system. For one, the surface served as a cathode, and for the other, an anode. The discharge current was varied from 30 to 70 mA. The setup scheme is described in more detail in [11].

The synthesized colloidal suspension was collected, then washed several times with distilled water, then subjected to air drying at a temperature of less than 60 °C.

The kinetics of the particle formation process was investigated using the method of turbidimetry. The intensity of the light passing through the layer (1 mm below the surface) of the solution was measured with an AvaSpec-2048 FT-2 spectrometer (Avantes, Netherlands). The optical length was 45 mm. The light source was a He-Ne laser (λ = 632.8 nm).

For qualitative and quantitative analysis of the phase composition of the powders, X-ray diffraction analysis was used (X-ray diffractometer DRON 3 M, Burevestnik, Russia, CuKa radiation). The diffraction patterns were processed using QualX2 software [12] and the open crystallographic COD database [13].

The shape of the particles, their sizes and elemental composition of the powder were obtained using scanning electron microscopy (SEM, Tesla Vega 3SBH, Czech Republic) with an EDX analysis system (Aztec EDS, Oxford Instruments Ltd., England).

The pH of the solution were measured before and after solution treatment using a PHT-028 multivariable water quality monitor (Kelilong, China).

The average hydrodynamic diameter of the formed particles was determined by dynamic light scattering (DLS) using a Photocor Compact-Z size analyzer (Photocor, Russia).

Thermogravimetric analysis (TGA) and differential scanning calorimetry (DSC) of the obtained precipitates were performed on a STA 449 F1 Jupiter thermal analysis instrument (Netzsch, Germany). The temperature range was 20 °C-800 °C at a heating rate of 5 °C min^{-1} in an argon flow using a platinum crucible.

RESULTS AND DISCUSSION

When a discharge acts on a solution, the following phenomena are visually observed. After about 2 min of discharge burning, the initial slightly yellow solution began to darken to a depth of about 1 cm in the anode cell. With increasing time, the darkening area begins to spread deep into the solution. Starting from 3-4 min in the darkening area, there is a loss of aggregate stability. Colloidal particles form larger agglomerates, which start to precipitate.

Let us estimate the pH of the initial solution and the degree of salt hydrolysis (α). Salt hydrolysis occurs mainly in the first stage, that is, according to the reaction:

$$Fe^{3+} + HOH \leftrightarrow FeOH^{2+} + H^+$$

Taking into account that $[OH^-]\cdot[H^+] = 10^{-14}$, the concentration of water molecules is equal to 55.6 mol/l and the instability constant of hydrocomplexes (the equilibrium constant of the reaction (1)) is equal to $1.35\cdot10^{-12}$ [14], we obtain that the hydrolysis constant (reaction (1)) is equal to $7.4\cdot10^{-3}$. The hydrolysis constant (K_h) is related to the degree of hydrolysis (α) by the ratio

$$K_h = \frac{\alpha^2 \cdot C}{1-\alpha}$$

where C is the concentration.

For a concentration of 5 mmol/l, the degree of hydrolysis was 0.684, and the pH of the solution was ~2.46. The experimentally measured pH value was 2.1. The solubility product (SP) of iron (III) hydroxide is $3.8\cdot10^{-38}$. From the expression $SP = [Fe^{3+}]\cdot[OH^-]=3.8\cdot10^{-38}$ it follows that at a concentration of $[Fe^{3+}]$ = 5 mmol/l the pH of the solution will be 2.3. Also, according to the handbook [11], the beginning of the precipitation of iron(III) hydroxide corresponds to pH ~ 2.3, and the complete precipitation of the precipitate can be observed already at pH = 4.1. That is, in an acidic environment, iron(III) hydroxides and insoluble basic salts, especially iron III hydroxosulfates), should be formed. Indeed, elemental analysis of uncalcined sediment samples showed that it consists of iron, oxygen, and sulfur in the ratio Fe : S: O = 4: 1: 17. The chemical composition of the sediment corresponding to this ratio can be represented by formula $(Fe(OH)_2)_2SO_4\cdot2Fe(OH)_3\cdot3H_2O$. The uncalcined powder showed no reflections in the X-ray spectrum. Therefore, it has an amorphous structure.

The results of thermogravimetric and differential thermogravimetric analyzes (calcination) are shown in Fig. 1. The first broad endothermic peak (100-250 °C) is apparently associated with the stepwise dehydration of iron sulfate by the reactions:

$$Fe_2(SO_4)_3\cdot3H_2O \rightarrow Fe_2(SO_4)_3\cdot2H_2O + H_2O$$
(~115-145 °C)

$$Fe_2(SO_4)_3\cdot2H_2O \rightarrow Fe_2(SO_4)_3\cdot H_2O + H_2O$$
(~145-170 °C)

...

$$Fe_2(SO_4)_3\cdot H_2O \rightarrow Fe_2(SO_4)_3 + H_2O$$
(~240-260 °C)

The peaks in the region of 500-700 °C can be associated with the occurrence of the following reactions:

$$Fe_2(SO_4)_3 \rightarrow Fe_2O_3 + 3\ SO_3$$
(~500-700 °C)

$$2Fe(OH)_3 \rightarrow Fe_2O_3 + 3\ H_2O$$
(~500-700 °C)

As shown by X-ray diffraction analysis (Fig. 2), the final product of calcination is crystalline γ -Fe_2O_3.

SEM images of the calcined and uncalcined powders are shown in Fig. 3. The uncalcined sediment has a rather dense structure. The size of individual particles is difficult to determine. But it can be seen that it is about 100 nm on average. The calcined sample also has a dense structure. A very developed surface is noteworthy, which is important for catalysis. The particle size is less than 50 nm on average.

The DLS data do not contradict the SEM data. According to the DLS results, the colloidal solution consists of two narrow fractions. The main fraction (73%) is represented by particles with a size of 46.6±4 nm. And the other fraction (27%) consists of 948±36 nm particles.

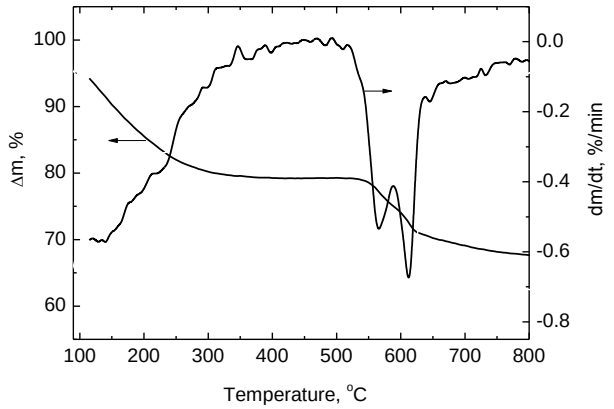

Fig. 1. Thermogravimetric and differential thermogravimetric curves of calcination of powders

Рис.1. Термогравиметрические и дифференциальные термогравиметрические кривые прокалки порошков

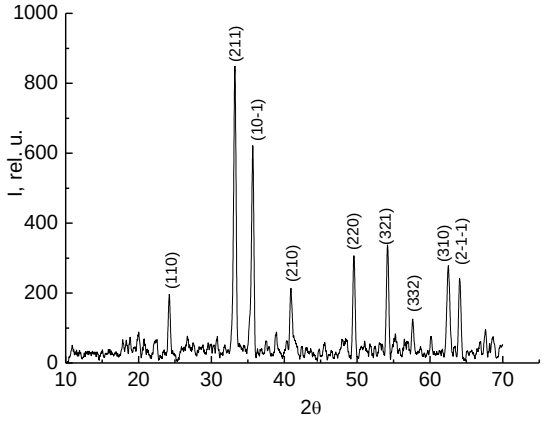

Fig. 2. X-ray diffraction pattern of the annealed powder. Final product of annealing is crystalline γ -Fe_2O_3 (hematite). The spectrum was decoded according to [15]

Рис. 2. Рентгенограмма порошка после отжига. Продукт отжига - γ -Fe_2O_3 (гематит). Расшифровка спектра проведена по данным работы [15]

Based on the above estimates, the initial solutions should already contain colloidal particles of hydroxosulfates and hydroxides. Under our conditions, the concentration of iron ions is much higher than the concentration of OH^- ions. That is, the reaction of the formation of hydroxides and hydroxosulfates, for example, by the reactions $nFe^{3+} + 1.5nSO_4^{2-} + 3mOH^- \rightarrow \rightarrow mFe(OH)_3\downarrow + 1.5nSO_4^{2-} + (n-m)Fe^{3+}$, and $nFe^{3+} + +1.5nSO_4^{2-} + OH^- \rightarrow mFe(OH)SO_4\downarrow + (1.5n-m)SO_4^{2-} + +(n-m)Fe^{3+}$ occur with an excess of iron ions. SO_4^{2-} ions can be potential-forming ions, and Fe^{3+} ions can be counterions. A micelle can have the form:

$$\{m[Fe(OH)_3]\ n[Fe(OH)SO_4]\ jSO_4^{2-}\ kH_2O\}^{-2j}$$

The presence of negatively charged micelles determines the specific shape of the turbidimetric kinetic curve (Fig. 4). When the discharge is turned on, two processes take place. The first process is the exit of micelles from the near-surface layer of the solution due to their drift in an electric field. The second process is the formation of micelles. The first process prevails at the initial exposure times and leads to a clarification of the solution. For a long time, the formation of micelles predominates over their escape, and the transmission of the solution decreases due to light scattering.

The rate of formation of the colloidal solution increased with increasing discharge current. In fig. 5 shows the dependence of the effective rate constant obtained from the slope of the second section of the kinetic curve.

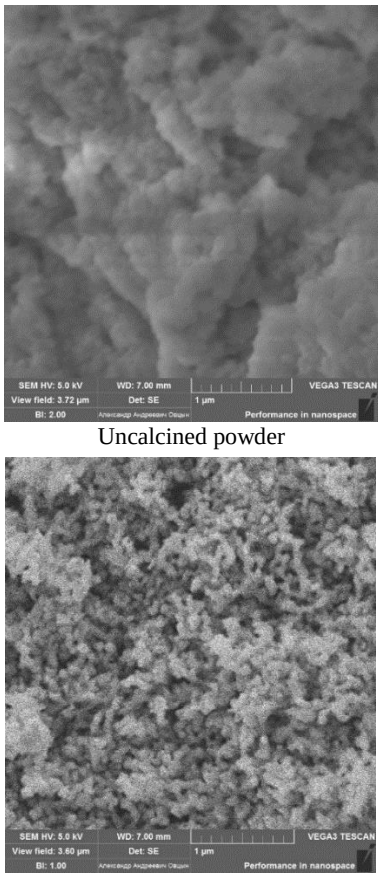

Fig. 3. SEM images of calcined and uncalcined powders

Рис. 3. СЭМ изображения прокаленного и не прокаленного порошков

From the point of view of chemistry, the observed phenomena can be explained as follows. It is well known that the impact of the discharge on the water cathode and the water anode leads to different results [16, 17]. The water in the cathode becomes acidic, and in the anode it becomes alkaline. For example, at a discharge current of 40 mA in an air atmosphere, the pH in the anode increases from 7 to 11, and in a liquid cathode, the pH decreases from 7 to 3 when the discharge operates for 300 s [13]. Apparently, the formation of an alkaline solution is associated with the following [18, 19]. The surface of the anode, unlike the cathode, is bombarded by a flux of electrons, which are

rapidly solvated. As a result, their concentration in a surface layer with a thickness of the order of several nanometers reaches a value of about 1 mmol/l. The main reaction of the decay of solvated electrons is their reaction with water molecules, leading to the formation of hydroxide ions, that is, the formation of an alkaline medium.

$H_2O + e_{solv} \rightarrow O + OH^-$ ($2K=1.1\cdot10^{10}$ l/(mol·s))

The rate of this reaction should increase with increasing discharge current which corresponds to the experiment (Fig. 5). Since the concentration of water molecules is higher than the concentration of metal ions by three orders of magnitude, the solvated electrons are consumed by reaction (1), and not for the reduction of ions. Indeed, the experiment shows that the pH of the solution in the anode cell increases with an increase in the processing time by the discharge. At the same time, pH decreases in the cathode cell. Thus, in a time of 300 s at a concentration of 5 mmol/l and a current of 50 mA in the anode cell, the pH increases from 2.1 to 3.2, and in the cathode cell, the pH drops from 2.1 to 1.8.

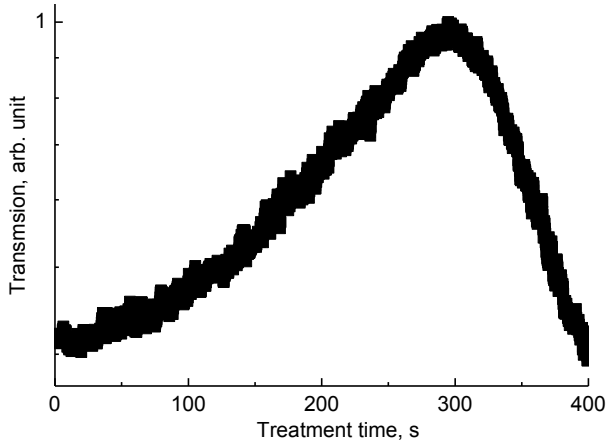

Fig. 4. Kinetic curve. Current is 50 mA. Concentration is 5 mmol/l
Рис. 4. Кинетическая кривая. Ток 50 мА. Концентрация 5 ммоль/л

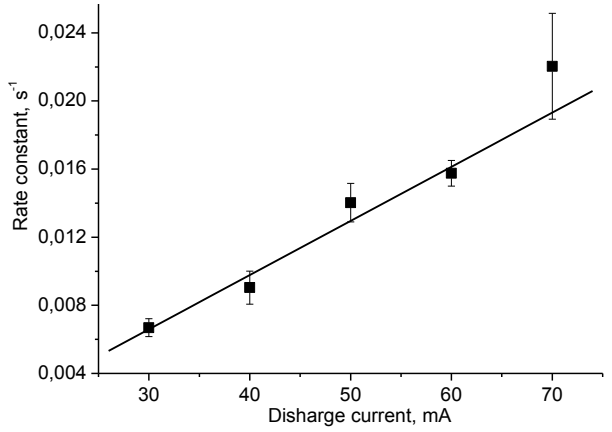

Fig. 5. The dependence of efficient rate constant on the discharge current/ Concentration is 5 mmol/l
Рис. 5. Зависимость эффективной константы скорости от тока разряда. Концентрация 5 ммоль/л

CONCLUSION

Thus, the formation of insoluble iron hydroxo compounds is due to the fact that the action of the discharge leads to the formation of solvated electrons in the anode part. In the reactions of electrons with water molecules, OH^- ions are formed, which leads to an increase in the pH of the solution and stimulates the formation of a colloidal solution consisting of iron hydroxides and hydroxosulfates. When these compounds are calcined, crystalline iron oxide (3) is obtained in γ form (hematite).

ACKNOWLEDGEMENTS

This work was supported by the Ministry of High Education and Science of the Russian Federation, project No FZZW-2020-0009.

Работа поддержана Министерством высшего образования и науки Российской Федерации, проект № FZZW-2020-0009.

REFERENCES
ЛИТЕРАТУРА

1. **Wang C., Diamon H., Sun S.** Dumbbell-like Pt−Fe_3O_4 Nanoparticles and Their Enhanced Catalysis for Oxygen Reduction Reaction. *Nano Lett.* 2009. V. 9. N 4. P. 1493-1496. DOI: 10.1021/nl8034724.
2. **Apostolescu N., Geiger B., Hizbullah K., Jan M.T., Kureti S., Reichert D., Schott F., Weisweiler W.** Selective catalytic reduction of nitrogen oxides by ammonia on iron oxide catalysts. *Appl. Catal. B: Environ.* 2001. V. 62. N 1-2. P. 104-114. DOI: 10.1016/j.apcatb.2005.07.004.
3. **Sreeram K.J., Indumathy R., Rajaram A., Nair B.U., Ramasami T.** Template synthesis of highly crystalline and monodisperse iron oxide pigments of nanosize. *Mater. Res. Bull.* 2006. V. 41. N 10. P. 1875-1881. DOI: 10.1016/j.materresbull.2006.03.017.
4. **Chen Q., Li J., Li Y.** A review of plasma–liquid interactions for nanomaterial synthesis. *J. Phys. D: Appl. Phys.* 2015. V. 48. N 28. P. 424005. DOI: 10.1088/0022-3727/48/42/424005.
5. **Saito G., Akiyama T.** Nanomaterial Synthesis Using Plasma Generation in Liquid 20. *J. Nanomater.* 2015. Article ID 123696. DOI: 10.1155/2015/123696.
6. **Shutov D.A., Rybkin V.V., Ivanov A.N., Smirnova K.V.** Synthesis of Zinc Oxide Powders in Plasma–Solution Systems. *High Energ. Chem.* 2017. V. 51. N 1. P. 65-69. DOI: 10.1134/S0018143917010118.
7. **Shutov D.A., Smirnova K.V., Gromov M.V., Rybkin V.V., Ivanov A.N.** Synthesis of CdO Ultradisperse Powders Using Atmospheric Pressure Glow Discharge in Contact With Solution and the Investigation of Intermediate Products. *Plasma Chem. Plasma Process.* 2018. V. 38. N 1. P. 107-121. DOI: 10.1007/s11090-017-9856-0.
8. **Шутов Д.А., Сунгурова А.В., Смирнова К.В., Манукян А.С., Рыбкин В.В.** Окислительно-восстановительные процессы с участием ионов марганца, инициируемые тлеющим разрядом, в водном растворе. *Изв. вузов. Химия и хим. технология*. 2018. Т. 61. Вып. 9-10. С. 23–29.

Shutov D.A., Sungurova A.V., Smirnova K.V., Manukyan A.S., Rybkin V.V. Oxidative-reducing processes with participation of manganese ions initiated by electric discharge in aqueous solution. *ChemChemTech [Izv. Vyssh. Uchebn. Zaved. Khim. Khim. Tekhnol.]*. 2018. V. 61. N 9-10. P. 24-30. DOI: 10.6060/ivkkt20186109-10.5802.

9. **Tochikubo F., Shirai N., Uchida S.** Liquid-phase reactions induced by atmospheric pressure glow discharge with liquid electrode. *J. Phys: Conf. Ser.* 2014. V. 565. P. 12010. DOI: 10.1088/1742-6596/565/1/012010.
10. **Khlyustova A., Sirotkin N., Titov V.** Plasma-induced precipitation of metal ions in aqueous solutions. *J. Chem. Technol. Biotechnol.* 2019. V. 94. N 12. P. 3987-3992. DOI: 10.1002/jctb.6204.
11. **Shutov D.A., Ivanov A.N., Rakovskaya A.V., Smirnova K.V., Manukyan A.S., Rybkin V.V.** Synthesis of oxygen-containing iron powders and water purification from iron ions by glow discharge of atmospheric pressure in contact with the solution. *J. Phys. D: Appl. Phys.* 2020. V. 53. N 28. P. 445202. DOI: 10.1088/1361-6463/aba4d7.
12. **Altomare A., Corriero N., Cuocci C., Falcicchio A., Moliterni A., Rizzi R.** QUALX2.0: a qualitative phase analysis software using the freely available database POW_COD. *J. Appl. Cryst.* 2015. V. 48. N 2. P. 598-603. DOI: 10.1107/S1600576715002319.
13. **Grazulis S., Daskevic A., Merkys A., Chateigner D., Lutterotti L., Quiros M., Serebryanaya N.R., Moeck P., Downs R.T., LeBail A.** Crystallography Open Database (COD): an open-access collection of crystal structures and platform for world-wide collaboration. *Nucl. Acids. Res.* 2012. V. 40. N D1. P. D420-427. DOI: 10.1093/nar/gkr900.
14. **Goronovsky I.T., Nazarenko Yu.P., Nekryach E.F.** A short guide to chemistry. Kiev: Naukova Dumka. 1987. 828 p. (in Russian). **Гороновский И.Т., Назаренко Ю.П., Некряч Е.Ф.** Краткий справочник по химии. Киев: Наукова Думка. 1987. 828 с.
15. **Pauling L., Hendricks S.B.** The crystal structures of hematite and corundum. *J. Am. Chem. Soc.* 1925. V. 47. N 3. P. 781-790. DOI: 10.1021/ja01680a027.
16. **Ivanov A.N., Shutov D.A., Manukyan A.S., Rybkin V.V.** Influence of Non‑uniformity of Generation of Active Particles on Deposition Processes and Redox Reactions in a Glow Discharge in Contact with Water. *Plasma Chem. Plasma Process.* 2019. V. 39. N 1. P. 63-73. DOI: 10.1007/s11090-018-9936-9.
17. **Witzke M., Rumbach P., Go D.B., Sankaran R.M.** Evidence for the electrolysis of water by atmospheric-pressure plasmas formed at the surface of aqueous solutions. *J. Phys. D: Appl. Phys.* 2012. V. 45. N 7. P. 442001. DOI: 10.1088/0022-3727/45/44/442001.
18. **Rumbach P., Bartels D.M., Sankaran R.M., Go D.B.** The solvation of electrons by an atmospheric-pressure plasma. *Nat. Comm.* 2015. V. 6. P. 7248. DOI: 10.1038/ncomms8248.
19. **Rumbach P., Bartels D.M., Go D.B.** The penetration and concentration of solvated electrons and hydroxyl radicals at a plasma-liquid interface. *Plasma Sours. Sci. Technol.* 2018. V. 27. N 11. P. 115013. DOI: 10.1088/1361-6595/aaed07.

Поступила в редакцию 25.01.2021
Принята к опубликованию 30.03.2021

Received 25.01.2021
Accepted 30.03.2021